

IPMU-11-0121

UT-11-23

KEK-TH-1478

LHC Test of CDF Wjj anomaly

Keisuke Harigaya^{1,2}, Ryosuke Sato^{1,2}, and Satoshi Shirai³

¹*Institute for the Physics and Mathematics of the Universe, University of Tokyo,
Kashiwa 277-8568, Japan*

²*Department of Physics, University of Tokyo,
Tokyo 113-0033, Japan*

³*Institute of Particle and Nuclear Studies,
High Energy Accelerator Research Organization (KEK)
Tsukuba 305-0801, Japan*

Abstract

We discuss a test of the CDF dijet anomaly at the LHC. The recent observed dijet mass peak at the CDF is well fitted by a new particle with a mass of around 150 GeV, which decays into two jets. In this paper, we focus on only Wjj signal to avoid model dependence, and comprehensively study the LHC discovery/exclusion reach. We found almost all the models are inconsistent with the result of the LHC, unless only valence quarks contribute the new process.

1 Introduction

Recently, the CDF collaboration reported an anomaly in Wjj events [1]. This result indicates a new particle X with mass around 150 GeV and the production cross section associated with a W boson is around 4 pb at the Tevatron. There are many models proposed to explain this anomaly [2, 3, 4, 5]. Since the D0 collaboration reports result inconsistent with the CDF [6], it is very important to test the Wjj anomaly at the LHC. Each model can have individual manner to be tested. Some model may predict the collider signals other than Wjj . For example, Ref. [7] discusses the testing at the LHC for the Technicolor model by using various modes. However, the discussion using modes other than Wjj is strongly model dependent. In this paper, we focus on only Wjj signal at the LHC to test various models with model independent manner, regardless of such other considerations. When we discuss the various models, we do not consider the flavor symmetry violation or the deviation from the electroweak precision test. To discuss them, we have to specify the whole of the model. Furthermore, some other particles unrelated to Wjj signal may compensate such a violation, then, the comprehensive study is difficult. We comprehensively study models which can realize Wjj signal at the Tevatron. We discussed the expected signal at the LHC and found that almost all models can be discovered or excluded at the LHC.

2 Setup

A lot of models proposed to explain the CDF dijet anomaly assume tree level s-channel or t-channel process¹ whose final state is a W boson and a new particle X with a mass of around 150 GeV. We considered two case.

- W boson and X are produced non-resonantly and X decays into two jet.
- another particle Y is produced by s-channel then it decays into a W boson and X .

For the former case, to test such models with model independent manners, we concentrate on the effective theory. We consider the cases in which the particle X is described by

¹ There are models which can not be classified to such a class. For example, in some models [4], new particles are pair-produced at first, and a W boson and jj are generated from each new particle decay.

scalar, spinor and vector field. We denote the particle as ϕ , V^μ , ψ for the case of scalar, vector and spinor particle respectively. We have considered possible effective operators to provide a process $p\bar{p} \rightarrow WX$ up to dimension 5. In constructing the effective operators, we have respected the $SU(3)_c \times SU(2)_L \times U(1)_Y$ gauge symmetry and the Lorentz symmetry but allowed the operators which can arise by the standard model higgs condensation.

For the latter case, a resonant behavior of Wjj signal is constrained from $m_{\ell\nu jj}$ distribution, but $m_{\ell\nu jj}$ peak around 280 GeV is less constrained [8]. In the following of this paper, we set the mass of Y to be 280 GeV when we consider the case WX is produced by s-channel resonance process. We have concentrated on the case in which the narrow width approximation is valid. In this way, we can give model-independent result.

We also assumed that the CP invariance is preserved and the hermiticity is preserved at the level of effective operators. That is, when an effective operator is introduced, its hermite conjugate operator is also introduced.

3 Constrains from hadron collider experiments

3.1 LHC

Here, we discuss the discovery/exclusion reach at the LHC 7 TeV run. The ATLAS group shows dijet invariant mass M_{jj} distribution associated with a W boson with 1.02 fb^{-1} data [9]. This data is consistent with background, then, it gives a severe constraint on the WX cross section at the LHC. The ATLAS groups shows the data with 3 jets veto and the data without veto. The data without 3 jets veto gives more severe constraint on the cross section, because 3 jets veto significantly decreases signal acceptance while the background can not be so reduced. In the following of this section, we use the data without 3 jets veto.

When the decay width of X is small enough compared to the jet resolution, WX events may give significant contribution to M_{jj} distribution around 150 GeV. We estimate signal acceptance for the event cut used in Ref. [9] by using MadGraph-Pythia-PGS package [10]. Given signal acceptance, we can estimate the upper bound of WX cross section by simple event number counting. We estimate the upper bound of WX cross section at 95% C.L. by using the RooStats tools [11]. We can get the upper bound as 16.7 pb from

Table 1: The upper bound of WX cross section at 95% C.L. in the LHC 7 TeV run. The row shows each integrated luminosity. The most bottom row shows the limit when statistical error can be neglect. The column shows the size of systematic error. In the left column we take the same systematic error as Ref. [9], In the middle column we take the half of the systematic error as Ref. [9], In the right column we take only statistical error.

	sys.err. = Ref. [9]	sys.err. = $\frac{1}{2}$ Ref. [9]	only stat.err.
1.02 fb^{-1}	16.7 pb	12.9 pb	11.1 pb
$1.02 \text{ fb}^{-1} \times 2$	15.9 pb	11.6 pb	9.3 pb
$1.02 \text{ fb}^{-1} \times 4$	15.4 pb	10.8 pb	7.9 pb
$1.02 \text{ fb}^{-1} \times \infty$	15.0 pb	10.0 pb	

the present ATLAS data. In Section 4 and 5, we discuss the LHC discovery / exclusion by using the ratio of cross section between at the LHC 7 TeV run and at the Tevatron. When we take the cross section at the Tevatron to be 2 pb conservatively, the ratio of cross section have to be lower than 8.4. This value gives stringent constraint on the model which gives Wjj signal. The more integrated luminosity and the less systematic error can give more severe upper bound. The result is given by Table 1.²

3.2 $S\bar{p}\bar{p}S$

Some model predicts the single production of X by the quark or gluon fusion at hadron colliders. Due to the low energy kinematical cut, low energy hadron collider can set good constraints on the production cross section of X decaying into dijet. We utilized the results of the UA2 collaboration[12], which give the constraints on the production cross section times the branching ratio to dijet of heavy vector boson and quark. There are two things to be noticed.

First, their analysis assumed the particular value for the decay width of the produced particle. However, the assumed width is smaller than the mass resolution, which is about 10 % of the mass of the parent particle. Therefore, we apply their constraints on the production cross section if the decay width is smaller than $150 \times 0.1 = 15 \text{ GeV}$.

Second, their analysis assumed the decay mode of the produced particle. Heavy vector

² We fixed signal acceptance when we estimate the bound of the cross section. In fact, signal acceptance is dependent on the particle property and its interaction. Roughly, its dependence is a few ten percent.

bosons are assumed to have the same decay mode as the corresponding standard model vector bosons. That means they can decay into heavy quarks like b quark. b quark further decays into other particles, giving away some of jet energy. This results in the existence of low energy tail in the dijet mass distribution, which lowers the sensitivity of dijet peak search. On the other hand, heavy quarks are assumed to decay into ug or dg . Energy loss due to decay does not occur. Since the exclusion of operators including b quark did not depend on which to choose in our analysis, we can safely use the result for heavy quark in order to constrain the effective operators.³ The upper limit for the production cross section of X is 80 pb at 90 % C.L. In the same way as the constraint from the ATLAS result, we take the cross section at the Tevatron to be 2 pb conservatively. The ratio of cross section have to be lower than 40.

4 Non-resonant production

We classify the effective operators by X 's spin and its coupling to standard model particles. Note that in the case W boson's interaction is same as that of the standard model, X must couple to the left-handed quarks. In this section and the next section, we estimate a cross section at the hadron colliders by convoluting a parton level cross section with parton distribution functions. We have used CTEQ 6.1 PDF [13].

4.1 $X = \phi$: scalar particle

4.1.1 Quark- Quark- ϕ

The possible operators are

$$\phi q_L^\dagger q_R, \phi q_L q_L^c \quad (1)$$

and their conjugates. We suppress the colour indexes, which must be summed up appropriately so that the $SU(3)_c$ invariance is preserved. These interaction terms give $W\phi$ signal by t-channel quark exchange diagrams. The magnitude of coupling constants required to accomplish the cross section of 4 pb at the Tevatron can be translated into the

³It is possible that the constraints using the result of heavy quark is tighter for operators including c , s quark.

decay width $\Gamma(\phi \rightarrow qq)$. When the dimension of ϕ as a representation of $SU(3)_c$ is give by N_ϕ , The cross section $\sigma(qq \rightarrow W\phi)$ is proportional to $N_\phi\Gamma(\phi \rightarrow qq)$. Combinations of two quarks coupling to ϕ and the required $N_\phi\Gamma(\phi \rightarrow qq)$ are summarized in Table 2. The leftmost column shows the left-handed quark coupling to ϕ and the uppermost line shows its pair. For example, the elements (\bar{u}, d) and (\bar{u}, \bar{d}) means the coupling $\phi u_L^\dagger d_R$ and $\phi u_L^\dagger d_L^c$ respectively.

The ratio of the production cross section of $W\phi$ at the LHC with $\sqrt{s} = 7$ TeV to that of at the Tevatron with $\sqrt{s} = 1.96$ TeV is shown in Table 3. The elements marked \circ and written in blue letters are NOT excluded by the ATLAS result at 95 % CL [9]. We also show the ratio of the production cross section of single ϕ at Sp \bar{p} S with $\sqrt{s} = 540$ GeV to the production cross section of $W\phi$ at the Tevatron with $\sqrt{s} = 1.96$ TeV in Table 4. As is mentioned in 3.2, we require that the decay width of ϕ is lower than 15 GeV when applying the exclusion criteria based on the predicted production cross section of ϕ at Sp \bar{p} S. Since the required width is lower for ϕ with higher multiplicity, the exclusion is more severe for ϕ which obeys higher dimension representation of $SU(3)_c$. The elements marked \bullet and written in red letters are excluded by the UA2 result at 90 % CL [12] for ϕ which obeys any representation of $SU(3)_c$. * and green letters are for 8 or $6(\bar{6})$ representation.

All the operators are excluded from the ATLAS result unless the operators are composed of only valence quarks and ϕ . Even for operators composed of valence quarks, some of them are excluded by the UA2 result.

4.1.2 Gluon- W boson - ϕ

The possible operators are

$$G_{\mu\nu}^a W^{\mu\nu} \phi^a \quad (2)$$

and its conjugate. These interaction terms give $W\phi$ signal by the diagrams shown in Fig. 1. The required decay width $\Gamma(\phi \rightarrow gW)$ to accomplish 4 pb at the Tevatron with $\sqrt{s} = 1.96$ TeV is 8.5×10^{-2} GeV. This corresponds to the cutoff Λ of 850 GeV with the normalization $\frac{1}{\Lambda} G_{\mu\nu}^a W^{\mu\nu} \phi^a$. The ratio of the production cross section of $W\phi$ at the LHC with $\sqrt{s} = 7$ TeV to that of at the Tevatron with $\sqrt{s} = 1.96$ TeV is 8.6. This is excluded

by the ATLAS result at 95 % CL [9].

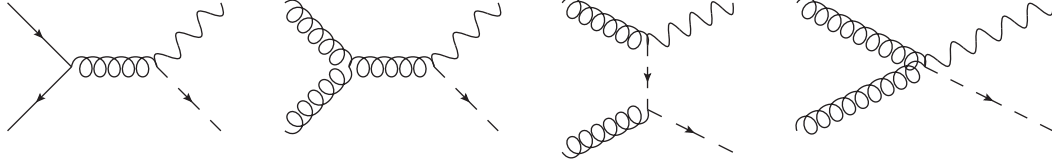


Figure 1: The diagrams contributing to the production of $W\phi$ by the operator $G_{\mu\nu}^a W^{\mu\nu} \phi^a$ at hadron colliders.

4.1.3 Photon or Z boson - W boson - ϕ

The possible operators are

$$B_{\mu\nu} W^{\mu\nu} \phi = (-\sin\theta_w Z_{\mu\nu} + \cos\theta_w F_{\mu\nu}) W^{\mu\nu} \phi \quad (3)$$

and its conjugate. These interaction terms give $W\phi$ signal by s-channel photon and Z boson exchange. The required decay width $\Gamma(\phi \rightarrow AW)$ to accomplish 4 pb at the Tevatron with $\sqrt{s} = 1.96$ TeV is 7.3 GeV. This corresponds to the cutoff Λ of 100 GeV with the normalization $\frac{1}{\Lambda} B_{\mu\nu} W^{\mu\nu} \phi$. The ratio of the production cross section of $W\phi$ at the LHC with $\sqrt{s} = 7$ TeV to that of at the Tevatron with $\sqrt{s} = 1.96$ TeV is 3.4. Though this is not excluded by the ATLAS result, cut off of 100 GeV is not acceptable as a higher dimensional operator.

We can think of an operator like $W_{\mu\nu} W^{\mu\nu} \phi$. However, such operator will result in an unacceptably lower cutoff, too.

4.2 $X = V$: vector particle

Since there are a lot of possible operators to explain the WV production at CDF, we pick up representative operators. Some variation of them are discussed in the text.

4.2.1 Quark - Quark - V : $V^\mu J_\mu$ type

The possible operators are

$$V^\mu q_L^\dagger \bar{\sigma}_\mu q_L, \quad V^\mu q_L^\dagger \bar{\sigma}_\mu q_R^c \quad (4)$$

and their conjugates. As in 4.1, we suppress the colour indexes. These interaction terms give $W\phi$ signal by t-channel quark exchange diagrams. The following analysis is same as that of 4.1. Combinations of two quarks coupling to V and the required $N_V\Gamma(V \rightarrow qq)$ are summarized in Table 5. Here, N_V is the dimension of V as a representation of $SU(3)_c$, and $\Gamma(V \rightarrow qq)$ is the decay width of $V \rightarrow qq$. The leftmost column shows the left-handed quark coupling to V and the uppermost line shows their pairs. For example, the elements (\bar{u}, d) and (\bar{u}, \bar{d}) mean the coupling $V^\mu u_L^\dagger \bar{\sigma}_\mu d_L$ and $V^\mu u_L^\dagger \bar{\sigma}_\mu d_R^c$ respectively.

The ratio of the production cross section of WV at the LHC with $\sqrt{s} = 7$ TeV to that of at the Tevatron with $\sqrt{s} = 1.96$ TeV is shown in Table 6. The elements marked \circ and written in blue letters are NOT excluded by the ATLAS result at 95 % CL [9]. We also show the ratio of the production cross section of single V at Sp \bar{p} S with $\sqrt{s} = 540$ GeV to the production cross section of WV at the Tevatron with $\sqrt{s} = 1.96$ TeV in Table 7. As is mentioned in 4.1.1, the exclusion based of the UA2 result depend on which $SU(3)_c$ representation V obeys. The elements marked \bullet and written in red letters are excluded by the UA2 result at 90 % CL [12] for V which obeys any representation of $SU(3)_c$. * and green letters are for 8 or $6(\bar{6})$ representation.

All the operators which do not contain valence quarks are excluded by the ATLAS result.

4.2.2 Quark - quark- V : Pauli term type

The possible operators are

$$V_{\mu\nu} q_L^c \sigma^{\mu\nu} q_L, \quad V_{\mu\nu} q_R^\dagger \sigma^{\mu\nu} q_L \quad (5)$$

and their conjugates where $\sigma^{\mu\nu} = \frac{i}{2}(\sigma^\mu \bar{\sigma}^\nu - \sigma^\nu \bar{\sigma}^\mu)$. As in 4.1, we suppress the colour indexes. These interaction terms give $W\phi$ signal by t-channel quark exchange diagrams. The following analysis is same as that of 4.1. Combinations of two quarks coupling to V and the required $N_V\Gamma(V \rightarrow qq)$ are summarized in Table 8. Here, N_V is the dimension of V as a representation of $SU(3)_c$, and $\Gamma(V \rightarrow qq)$ is the decay width of $V \rightarrow qq$. The leftmost column shows the left-handed quark coupling to V and the uppermost line shows their pairs. For example, the elements (\bar{u}, d) and (\bar{u}, \bar{d}) mean the coupling $V^{\mu\nu} u_L^\dagger \bar{\sigma}_{\mu\nu} d_R$ and $V^{\mu\nu} u_L^\dagger \bar{\sigma}_{\mu\nu} d_L^c$ respectively.

This can be also expressed in terms of the strength of the coupling. We have shown the required cut off Λ in Table 9 with the normalization

$$\frac{\sqrt{3}}{\sqrt{N_V}\Lambda} C_{ij}^r V_{\mu\nu}^r q_i^\dagger \sigma^{\mu\nu} q_j, \quad (6)$$

where q is two component quark field, i, j are the indexes of the color of quarks, r is the index of color of V , C_{ij}^r is the Clebsch-Gordan coefficients of the expansion $3(\bar{3}) \otimes 3(\bar{3})$ to the representation of $SU(3)_c$ which V obeys.

The ratio of the production cross section of WV at the LHC with $\sqrt{s} = 7$ TeV to that of at the Tevatron with $\sqrt{s} = 1.96$ TeV is shown in Table 10. The elements marked \circ and written in blue letters are NOT excluded by the ATLAS result at 95 % CL [9]. We also show the ratio of the production cross section of single V at Sp \bar{p} S with $\sqrt{s} = 540$ GeV to the production cross section of WV at the Tevatron with $\sqrt{s} = 1.96$ TeV in Table 11. As is mentioned in 4.1.1, the exclusion based of the UA2 result depend on which $SU(3)_c$ representation V obeys. The elements marked \bullet and written in red letters are excluded by the UA2 result at 90 % CL [12] for ϕ which obeys any representation of $SU(3)_c$. * and green letters are for 8 or $6(\bar{6})$.

All the operators which do not contain valence quarks are excluded by the ATLAS result.

4.2.3 Gluon - W boson - V

The possible operators are

$$G_{\mu\nu}^a W^\mu V^{a\nu} \quad (7)$$

and its conjugate. These interaction terms give $W\phi$ signal by the diagrams shown in Fig. 2. The required decay width $\Gamma(V \rightarrow gW)$ is 3.4×10^{-2} GeV. The ratio of the production cross section of $W\phi$ at the LHC with $\sqrt{s} = 7$ TeV to that of at the Tevatron with $\sqrt{s} = 1.96$ TeV is 1.4×10^1 . This is excluded by the ATLAS result at 95 % CL [9].

4.2.4 Photon or Z boson - W boson - V

The possible operators are

$$W_{\mu\nu}^3 W^\mu V^\nu = (\cos\theta_w Z_{\mu\nu} + \sin\theta_w F_{\mu\nu}) W^\mu V^\nu \quad (8)$$

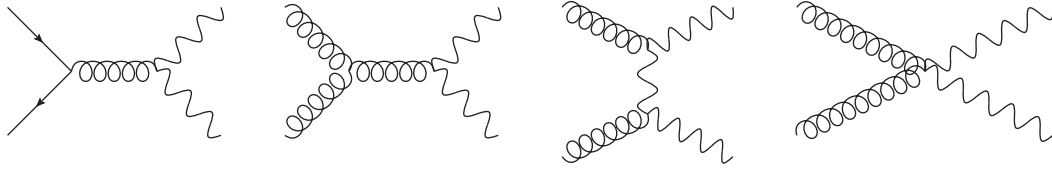


Figure 2: The diagrams contributing to the production of WV by the operator $G_{\mu\nu}^a W^\mu V^{a\nu}$ at hadron colliders.

and its conjugate. These interaction terms give WV signal by s-channel photon and Z boson exchange. The required decay width $\Gamma(V \rightarrow gW)$ is 1.1 GeV. The ratio of the production cross section of $W\phi$ at the LHC with $\sqrt{s} = 7$ TeV to that of at the Tevatron with $\sqrt{s} = 1.96$ TeV is 6.8. This value is allowed by the ATLAS result at 95 % CL [9].

We can think of operators like $W_{\mu\nu} W_\mu^3 V_\nu$, $B_{\mu\nu} W^\mu V^\nu$. These operators result in the similar cross section ratio. Therefore, such operators are still allowed, too.

4.3 $X = \psi$: spinor particle

4.3.1 Gluon - quark - ψ

The possible operators are

$$G_{\mu\nu} q_L^{c\dagger} \sigma^{\mu\nu} \psi_L \quad (9)$$

and their conjugates. As in 4.1, we suppress the colour indexes. These interaction terms give $W\phi$ signal by t-channel quark exchange diagrams. The following analysis is same as that of 4.1. Combinations of two particles coupling to ψ and the required $N_\psi \Gamma(\psi \rightarrow qg)$ are summarized in Table 12. Here, N_ψ is the dimension of ψ as a representation of $SU(3)_c$, and $\Gamma(\psi \rightarrow qg)$ is the decay width of $\psi \rightarrow qg$. The upper line shows the left-handed quark coupling to ψ . For example, the elements (g, u) and (g, \bar{u}) mean the coupling $G_{\mu\nu} u_L^{c\dagger} \sigma^{\mu\nu} \psi$ and $G_{\mu\nu} d_R^\dagger \sigma^{\mu\nu} \psi$ respectively. The corresponding cut off Λ is shown in Table 13 in GeV with the normalization

$$\frac{2}{\sqrt{N_\psi} \Lambda} C_{ai}^r G_{\mu\nu}^a q_i^\dagger \sigma^{\mu\nu} \psi_L^r, \quad (10)$$

where q is the two component quark field, i is the index of the color of quark, r is the index of the color of ψ and C_{ai}^r is the Clebsch-Gordan coefficients of the expansion $8 \otimes 3(\bar{3})$

to the representation of $SU(3)_c$ which ψ obeys.

The ratio of the production cross section of $W\psi$ at the LHC with $\sqrt{s} = 7$ TeV to that of at the Tevatron with $\sqrt{s} = 1.96$ TeV is shown in Table 14. All the operators are excluded by the ATLAS result at 95 % CL [9]. We also show the ratio of the production cross section of single ψ at Sp \bar{p} S with $\sqrt{s} = 540$ GeV to the production cross section of $W\psi$ at the Tevatron with $\sqrt{s} = 1.96$ TeV in Table 15. As is mentioned in 4.1.1, the exclusion based of the UA2 result depend on which $SU(3)_c$ representation V obeys. The elements marked \bullet and written in red letters are excluded by the UA2 result at 90 % CL [12] for ψ which obeys any representation of $SU(3)_c$. * and green letters are for $6(\bar{6})$ or 15 representation.

We can think of operators like $W^\mu q^\dagger \sigma_\mu \psi$. However, since gluon is necessary for initial state in order to produce $W\psi$, such operator will result in exclusion by the ATLAS result, too.

5 Resonant production

In calculating the production cross section, we use the narrow width approximation⁴, in which the parton level cross section is given by

$$\sigma(AB \rightarrow Y) = 16\pi^2 \frac{N_Y}{N_A N_B} \frac{\Gamma(Y \rightarrow AB)}{m_Y} \delta(s - m_Y^2) \quad (11)$$

where N is the degree of freedom of the particle, s is the square of the center of momentum. In this approximation, the combinations of two initial particle and the cross section at Tevatron with $\sqrt{s} = 1.96$ TeV is given in Table 16. Here, we have set the decay width to be 1 GeV. The ratio of the production cross section of Y at the LHC with $\sqrt{s} = 7$ TeV to that of at the Tevatron with $\sqrt{s} = 1.96$ TeV is shown in Table 17. The elements marked \circ and written in blue letters are NOT excluded by the ATLAS result at 95 % CL [9].

The operators including only valence quark are not excluded by the ATLAS result.

⁴The required decay width to accomplish 4 pb at the Tevatron with $\sqrt{s} = 1.96$ TeV might go beyond the validity of the narrow width approximation. In such a case, as is shown later, the ratio of the production cross section of Y at the LHC with $\sqrt{s} = 7$ TeV to that of at the Tevatron with $\sqrt{s} = 1.96$ TeV is greater than 40. Since such operators are excluded by ATLAS result, we do not have to consider such operators from the beginning.

Table 2: $(\phi q_L^i q^j, 4.1.1)$ Combinations of two quarks coupling to ϕ and $N_\phi \Gamma(\phi \rightarrow qq)$ in GeV required to accomplish 4 pb at the Tevatron with $\sqrt{s} = 1.96$ TeV. Here, N_ϕ is the dimension of ϕ as a representation of $SU(3)_c$, and $\Gamma(\phi \rightarrow qq)$ is the decay width of $\phi \rightarrow qq$.

$i \backslash j$	\bar{b}	\bar{c}	\bar{s}	\bar{u}	\bar{d}
b	5.3×10^5	9.7×10^2	9.1×10^2	1.9×10^2	8.3×10^1
\bar{c}	9.7×10^2	2.8×10^2	2.3×10^2	2.1×10^1	2.7×10^1
\bar{s}	9.1×10^2	2.3×10^2	1.6×10^2	2.6×10^1	2.2×10^1
\bar{u}	1.9×10^2	2.1×10^1	2.6×10^1	6.8	9.9
d	8.3×10^1	2.7×10^1	2.2×10^1	9.9	6.9
d	8.3×10^1	5.0×10^1	3.1×10^1	1.8	3.8
u	1.9×10^2	1.2×10^2	7.0×10^1	3.8	8.4
s	9.1×10^2	5.4×10^2	3.3×10^2	2.0×10^1	4.4×10^1
c	9.7×10^2	5.6×10^2	3.4×10^2	2.1×10^1	4.6×10^1
b	1.1×10^6	6.2×10^5	3.7×10^5	2.3×10^4	5.2×10^4

Table 3: $(\phi q_L^i q^j, 4.1.1)$ Combinations of two quarks coupling to ϕ and the ratio of the production cross section of $W\phi$ at the LHC with $\sqrt{s} = 7$ TeV to that of at the Tevatron with $\sqrt{s} = 1.96$ TeV. The elements marked \circ and written in blue letters are NOT excluded by the ATLAS result.

$i \backslash j$	\bar{b}	\bar{c}	\bar{s}	\bar{u}	\bar{d}
b	6.5×10^1	5.9×10^1	4.8×10^1	3.8×10^1	2.9×10^1
\bar{c}	5.9×10^1	5.3×10^1	4.5×10^1	2.4×10^1	2.7×10^1
\bar{s}	4.8×10^1	4.5×10^1	3.8×10^1	2.7×10^1	2.4×10^1
\bar{u}	3.8×10^1	2.4×10^1	2.7×10^1	3.0×10^1	2.4×10^1
d	2.9×10^1	2.7×10^1	2.4×10^1	2.4×10^1	3.0×10^1
d	2.9×10^1	2.6×10^1	2.1×10^1	$\circ 2.9$	$\circ 5.0$
u	3.8×10^1	3.4×10^1	2.8×10^1	$\circ 5.1$	$\circ 8.0$
s	4.8×10^1	4.3×10^1	3.8×10^1	1.2×10^1	1.6×10^1
c	5.9×10^1	5.3×10^1	4.7×10^1	1.6×10^1	2.2×10^1
b	6.5×10^1	5.9×10^1	5.3×10^1	2.1×10^1	2.7×10^1

Table 4: $(\phi q_L^i q^j, 4.1.1)$ Combinations of two quarks coupling to ϕ and the ratio of the production cross section of single ϕ at Sp \bar{p} S with $\sqrt{s} = 540$ GeV to the production cross section of $W\phi$ at the Tevatron with $\sqrt{s} = 1.96$ TeV. The elements marked \bullet and written in red letters and those marked $*$ and written in green letters are excluded by UA2 result at 90 % CL. For the difference between \bullet and $*$, see the text.

$i \backslash j$	\bar{b}	\bar{c}	\bar{s}	\bar{u}	\bar{d}
b	7.4×10^3	1.3×10^1	2.0×10^1	1.1×10^2	1.8×10^1
\bar{c}	1.3×10^1	1.5×10^1	10	2.3×10^1	1.1×10^1
\bar{s}	2.0×10^1	10	2.4×10^1	$* 4.9 \times 10^1$	1.6×10^1
\bar{u}	1.1×10^2	2.3×10^1	$* 4.9 \times 10^1$	$\bullet 7.3 \times 10^1$	$\bullet 4.3 \times 10^1$
d	1.8×10^1	1.1×10^1	1.6×10^1	$\bullet 4.3 \times 10^1$	3.2×10^1
d	1.8×10^1	2.1×10^1	2.2×10^1	$\bullet 4.2 \times 10^1$	3.6×10^1
u	1.2×10^2	1.3×10^2	1.3×10^2	$\bullet 2.1 \times 10^2$	$* 2.0 \times 10^2$
s	2.0×10^1	2.3×10^1	2.4×10^1	3.8×10^1	3.1×10^1
c	1.3×10^1	1.5×10^1	1.5×10^1	2.2×10^1	1.9×10^1
b	7.4×10^3	8.4×10^3	8.4×10^3	1.4×10^4	1.1×10^4

Table 5: $(V_\mu q_L^i \sigma^\mu q^j, 4.2.1)$ Combinations of two quarks coupling to V and $N_V \Gamma(V \rightarrow qq)$ in GeV required to accomplish 4 pb at the Tevatron with $\sqrt{s} = 1.96$ TeV. Here, N_V is the dimension of V as a representation of $SU(3)_c$, and $\Gamma(V \rightarrow qq)$ is the decay width of $V \rightarrow qq$.

$i \backslash j$	\bar{b}	\bar{c}	\bar{s}	\bar{u}	\bar{d}
b	2.5×10^5	4.5×10^2	4.2×10^2	8.9×10^1	3.8×10^1
\bar{c}	4.5×10^2	1.3×10^2	9.1×10^1	9.7	1.2×10^1
\bar{s}	4.2×10^2	9.1×10^1	7.6×10^1	1.1×10^1	1.0×10^1
\bar{u}	8.9×10^1	9.7	1.1×10^1	3.1	3.5
d	3.8×10^1	1.2×10^1	1.0×10^1	3.5	3.2
d	3.8×10^1	2.3×10^1	1.4×10^1	7.6×10^{-1}	1.7
u	9.0×10^1	5.3×10^1	3.2×10^1	1.7	3.7
s	4.2×10^2	2.5×10^2	1.5×10^2	8.6	1.9×10^1
c	4.5×10^2	2.6×10^2	1.6×10^2	9.2	2.1×10^1
b	5.0×10^5	2.9×10^5	1.7×10^5	1.0×10^4	2.4×10^4

Table 6: ($V_\mu q_L^i \sigma^\mu q^j$, 4.2.1) Combinations of two quarks coupling to V and the ratio of the production cross section of WV at the LHC with $\sqrt{s} = 7$ TeV to that of at the Tevatron with $\sqrt{s} = 1.96$ TeV. The elements marked \circ and written in blue letters are NOT excluded by the ATLAS result.

$i \backslash j$	\bar{b}	\bar{c}	\bar{s}	\bar{u}	\bar{d}
b	9.1×10^1	8.3×10^1	6.7×10^1	5.3×10^1	4.2×10^1
\bar{c}	8.3×10^1	7.5×10^1	5.4×10^1	3.6×10^1	3.8×10^1
\bar{s}	6.7×10^1	5.4×10^1	5.4×10^1	3.8×10^1	3.6×10^1
\bar{u}	5.3×10^1	3.6×10^1	3.8×10^1	5.3×10^1	3.0×10^1
d	4.2×10^1	3.8×10^1	3.6×10^1	3.0×10^1	5.4×10^1
d	4.2×10^1	3.7×10^1	3.1×10^1	$\circ 4.0$	$\circ 7.1$
u	5.4×10^1	4.8×10^1	4.1×10^1	$\circ 7.2$	1.1×10^1
s	6.7×10^1	6.1×10^1	5.4×10^1	1.7×10^1	2.3×10^1
c	8.3×10^1	7.5×10^1	6.6×10^1	2.4×10^1	3.1×10^1
b	9.1×10^1	8.3×10^1	7.5×10^1	3.0×10^1	3.9×10^1

Table 7: ($V_\mu q_L^i \sigma^\mu q^j$, 4.2.1) Combinations of two quarks coupling to V and the ratio of the production cross section of single V at Sp̄pS with $\sqrt{s} = 540$ GeV to the production cross section of WV at the Tevatron with $\sqrt{s} = 1.96$ TeV. The elements written in red or green letters are excluded by UA2 result at 90 % CL. For the difference between \bullet and $*$, see the text.

$i \backslash j$	\bar{b}	\bar{c}	\bar{s}	\bar{u}	\bar{d}
b	5.2×10^3	5.4×10^3	5.9×10^3	1.1×10^4	9.4×10^3
\bar{c}	9.2	1.0×10^1	9.6	1.9×10^1	1.6×10^1
\bar{s}	1.4×10^1	1.6×10^1	1.6×10^1	$* 5.1 \times 10^1$	3.8×10^1
\bar{u}	8.0×10^1	8.7×10^1	$* 9.2 \times 10^1$	$\bullet 5.0 \times 10^1$	$\bullet 6.6 \times 10^1$
d	1.3×10^1	1.4×10^1	1.5×10^1	3.5×10^1	2.2×10^1
d	1.3×10^1	6.8	8.7	2.2×10^1	1.2×10^1
u	7.9×10^1	1.3×10^1	1.9×10^1	$\bullet 6.8 \times 10^1$	2.2×10^1
s	1.4×10^1	6.3	8.2	1.9×10^1	8.7
c	9.2	5.1	6.3	1.3×10^1	6.8
b	2.6×10^3	9.2	1.4×10^1	7.9×10^1	1.3×10^1

Table 8: ($V_{\mu\nu}q_L^i\sigma^{\mu\nu}q^j$, 4.2.2) Combinations of two quarks coupling to V and $N_V\Gamma(V \rightarrow qq)$ in GeV required to accomplish 4 pb at the Tevatron with $\sqrt{s} = 1.96$ TeV. Here, N_V is the dimension of V as a representation of $SU(3)_c$, and $\Gamma(V \rightarrow qq)$ is the decay width of $V \rightarrow qq$.

$i \backslash j$	\bar{b}	\bar{c}	\bar{s}	\bar{u}	\bar{d}
b	6.8×10^4	1.2×10^2	1.1×10^2	2.4×10^1	1.0×10^1
\bar{c}	1.2×10^2	3.6×10^1	3.2×10^1	2.6	3.3
\bar{s}	1.1×10^2	3.2×10^1	2.0×10^1	3.2	2.7
\bar{u}	2.4×10^1	2.6	3.2	8.2×10^{-1}	1.4
d	1.0×10^1	3.3	2.7	1.4	8.3×10^{-1}
d	1.0×10^1	6.0	3.7	1.8×10^{-1}	4.2×10^{-1}
u	2.4×10^1	1.4×10^1	8.7	4.1×10^{-1}	9.5×10^{-1}
s	1.1×10^2	6.7×10^1	4.1×10^1	2.2	5.0
c	1.2×10^2	7.2×10^1	4.3×10^1	2.4	5.6
b	1.4×10^5	7.8×10^4	4.8×10^4	2.7×10^3	6.3×10^3

Table 9: ($V_{\mu\nu}q_L^i\sigma^{\mu\nu}q^j$, 4.2.2) Combinations of two quarks coupling to V and cut off Λ in GeV required to accomplish 4 pb at the Tevatron with $\sqrt{s} = 1.96$ TeV. See the text for the definition of Λ .

$i \backslash j$	\bar{b}	\bar{c}	\bar{s}	\bar{u}	\bar{d}
b	1.4	4.7×10^1	4.9×10^1	1.1×10^2	1.6×10^2
\bar{c}	4.7×10^1	6.1×10^1	9.2×10^1	3.2×10^2	2.8×10^2
\bar{s}	4.9×10^1	9.2×10^1	8.1×10^1	2.9×10^2	3.2×10^2
\bar{u}	1.1×10^2	3.2×10^2	2.9×10^2	4.0×10^2	4.4×10^2
d	1.6×10^2	2.8×10^2	3.2×10^2	4.4×10^2	4.0×10^2
d	1.6×10^2	2.1×10^2	2.7×10^2	1.2×10^3	8.0×10^2
u	1.1×10^2	1.4×10^2	1.8×10^2	8.1×10^2	5.3×10^2
s	4.9×10^1	6.4×10^1	8.1×10^1	3.5×10^2	2.3×10^2
c	4.7×10^1	6.1×10^1	7.9×10^1	3.4×10^2	2.2×10^2
b	1.4	1.9	2.4	10	6.5

Table 10: ($V_{\mu\nu}q_L^i\sigma^{\mu\nu}q^j$, 4.2.2) Combinations of two quarks coupling to V and the ratio of the production cross section of WV at the LHC with $\sqrt{s} = 7$ TeV to that of at the Tevatron with $\sqrt{s} = 1.96$ TeV. The elements marked \circ and written in blue letters are NOT excluded by the ATLAS result.

$i \backslash j$	\bar{b}	\bar{c}	\bar{s}	\bar{u}	\bar{d}
b	9.5×10^1	8.8×10^1	7.2×10^1	6.0×10^1	4.8×10^1
\bar{c}	8.8×10^1	8.0×10^1	5.1×10^1	4.3×10^1	4.4×10^1
\bar{s}	7.2×10^1	5.1×10^1	5.9×10^1	4.4×10^1	4.4×10^1
\bar{u}	6.0×10^1	4.3×10^1	4.4×10^1	7.5×10^1	3.8×10^1
d	4.8×10^1	4.4×10^1	4.4×10^1	3.8×10^1	7.6×10^1
d	4.8×10^1	4.3×10^1	3.7×10^1	$\circ 4.5$	$\circ 8.2$
u	6.0×10^1	5.4×10^1	4.7×10^1	$\circ 8.3$	1.3×10^1
s	7.2×10^1	6.5×10^1	5.9×10^1	1.9×10^1	2.5×10^1
c	8.8×10^1	8.0×10^1	7.2×10^1	2.8×10^1	3.6×10^1
b	9.5×10^1	8.6×10^1	7.9×10^1	3.4×10^1	4.3×10^1

Table 11: ($V_{\mu\nu}q_L^i\sigma^{\mu\nu}q^j$, 4.2.2) Combinations of two quarks coupling to V and the ratio of the production cross section of single V at Sp̄pS with $\sqrt{s} = 540$ GeV to the production cross section of WV at the Tevatron with $\sqrt{s} = 1.96$ TeV. The elements written in red or green letters are excluded by UA2 result at 90 % CL. For the difference between \bullet and $*$, see the text.

$i \backslash j$	\bar{b}	\bar{c}	\bar{s}	\bar{u}	\bar{d}
b	2.8×10^3	5.1	7.6	$* 4.3 \times 10^1$	6.7
\bar{c}	5.1	5.6	4.2	8.4	4.1
\bar{s}	7.6	4.2	8.8	1.8×10^1	5.7
\bar{u}	$* 4.3 \times 10^1$	8.4	1.8×10^1	2.6×10^1	1.8×10^1
d	6.7	4.1	5.7	1.8×10^1	1.2×10^1
d	6.7	7.5	7.9	1.3×10^1	1.2×10^1
u	$* 4.3 \times 10^1$	$* 4.7 \times 10^1$	$* 5.0 \times 10^1$	$\bullet 6.8 \times 10^1$	$\bullet 6.7 \times 10^1$
s	7.6	8.7	8.8	1.2×10^1	1.1×10^1
c	5.1	5.6	5.7	7.8	6.9
b	2.8×10^3	3.2×10^3	3.2×10^3	4.8×10^3	4.1×10^3

Table 12: ($G_{\mu\nu}q^\dagger\sigma^{\mu\nu}\psi$, 4.3.1) Combinations of two particles coupling to ψ and $N_\psi\Gamma(\psi \rightarrow qq)$ in GeV required to accomplish 4 pb at the Tevatron with $\sqrt{s} = 1.96$ TeV. Here, N_ψ is the dimension of ψ as a representation of $SU(3)_c$, and $\Gamma(\psi \rightarrow qq)$ is the decay width of $\psi \rightarrow qq$.

	b	\bar{c}	\bar{s}	\bar{u}	d
g	3.1×10^1	1.8×10^1	1.1×10^1	6.7×10^{-1}	1.6

Table 13: ($G_{\mu\nu}q^\dagger\sigma^{\mu\nu}\psi$, 4.3.1) Combinations of two particles coupling to ψ and cut off Λ in GeV required to accomplish 4 pb at the Tevatron with $\sqrt{s} = 1.96$ TeV. See the text for the definition of Λ .

	b	\bar{c}	\bar{s}	\bar{u}	d
g	1.9×10^2	2.4×10^2	3.1×10^2	1.3×10^3	8.3×10^2

Table 14: ($G_{\mu\nu}q^\dagger\sigma^{\mu\nu}\psi$, 4.3.1) Combinations of two particles coupling to ψ and the ratio of the production cross section of $W\psi$ at the LHC with $\sqrt{s} = 7$ TeV to that of at the Tevatron with $\sqrt{s} = 1.96$ TeV

	b	\bar{c}	\bar{s}	\bar{u}	d
g	9.5×10^1	8.7×10^1	7.9×10^1	3.8×10^1	4.8×10^1

Table 15: ($G_{\mu\nu}q^\dagger\sigma^{\mu\nu}\psi$, 4.3.1) Combinations of two particles coupling to ψ and the ratio of the production cross section of single ψ at Sp̄pS with $\sqrt{s} = 540$ GeV to the production cross section of $W\psi$ at the Tevatron with $\sqrt{s} = 1.96$ TeV. The elements written in red or green letters are excluded by UA2 result at 90 % CL. For the difference between \bullet and $*$, see the text.

	b	\bar{c}	\bar{s}	\bar{u}	d
g	$* 2.1 \times 10^2$	$\bullet 2.4 \times 10^2$	$\bullet 2.4 \times 10^2$	$\bullet 3.5 \times 10^2$	$\bullet 3.2 \times 10^2$

Table 16: (Resonance, 5) Combinations of two particles coupling to Y and the production cross section of Y in pb when the decay width of Y to the two particles is 1 GeV at the Tevatron with $\sqrt{s} = 1.96$ TeV.

	b	\bar{c}	\bar{s}	\bar{u}	d	g
b	6.0×10^{-2}	1.0×10^{-1}	1.7×10^{-1}	2.6	1.2	9.6×10^{-1}
\bar{c}	1.0×10^{-1}	1.8×10^{-1}	3.0×10^{-1}	4.2	1.9	1.7
\bar{s}	1.7×10^{-1}	3.0×10^{-1}	5.0×10^{-1}	6.9	3.2	2.7
\bar{u}	2.6	4.2	6.9	1.8×10^1	1.5×10^1	3.7×10^1
d	1.2	1.9	3.2	1.5×10^1	9.7	1.7×10^1
g	9.6×10^{-1}	1.7	2.7	3.7×10^1	1.7×10^1	1.5×10^1
d	1.2	1.9	3.2	4.3×10^1	2.2×10^1	1.7×10^1
u	2.6	4.2	6.9	8.2×10^1	4.3×10^1	3.7×10^1
s	1.7×10^{-1}	3.0×10^{-1}	5.0×10^{-1}	6.9	3.2	2.7
c	1.0×10^{-1}	1.8×10^{-1}	3.0×10^{-1}	4.2	1.9	1.7
b	6.0×10^{-2}	1.0×10^{-1}	1.7×10^{-1}	2.6	1.2	9.6×10^{-1}

Table 17: (Resonance, 5) Combinations of two particles coupling to Y and the ratio of the production cross section of Y at the LHC with $\sqrt{s} = 7$ TeV to that of at the Tevatron with $\sqrt{s} = 1.96$ TeV. The elements marked \circ and written in blue letters are NOT excluded by the ATLAS result.

	b	\bar{c}	\bar{s}	\bar{u}	d	g
b	7.4×10^1	6.7×10^1	5.8×10^1	2.2×10^1	2.9×10^1	6.1×10^1
\bar{c}	6.7×10^1	6.1×10^1	5.2×10^1	1.9×10^1	2.6×10^1	5.5×10^1
\bar{s}	5.8×10^1	5.2×10^1	4.4×10^1	1.5×10^1	2.1×10^1	4.7×10^1
\bar{u}	2.2×10^1	1.9×10^1	1.5×10^1	1.7×10^1	1.5×10^1	1.8×10^1
d	2.9×10^1	2.6×10^1	2.1×10^1	1.5×10^1	1.6×10^1	2.4×10^1
g	6.1×10^1	5.5×10^1	4.7×10^1	1.8×10^1	2.4×10^1	5.0×10^1
d	2.9×10^1	2.6×10^1	2.1×10^1	$\circ 4.1$	$\circ 6.2$	2.4×10^1
u	2.2×10^1	1.9×10^1	1.5×10^1	$\circ 2.6$	$\circ 4.1$	1.8×10^1
s	5.8×10^1	5.2×10^1	4.4×10^1	1.5×10^1	2.1×10^1	4.7×10^1
c	6.7×10^1	6.1×10^1	5.2×10^1	1.9×10^1	2.6×10^1	5.5×10^1
b	7.4×10^1	6.7×10^1	5.8×10^1	2.2×10^1	2.9×10^1	6.1×10^1

6 Conclusion and Discussion

In this paper, we discuss testability of the CDF Wjj anomaly at the LHC. We comprehensively study models which can realize Wjj signal observed by the CDF collaboration. We have found that the cross section at the LHC mainly depends on what partons in p and \bar{p} produce W and X and that almost all the models are inconsistent with the result of the LHC, unless only valence quarks contribute the new process. Even in such a case, if the systematic uncertainty of estimation of the standard model background is sufficiently suppressed, it is possible to discover/exclude the Wjj signal. Although, as mentioned in footnote 1, some models are not within our study. However, even in such a case, the cross section at the LHC is expected to be $\mathcal{O}(1) \times \sigma_{\text{Tevatron}}$ in the case of production by valence quarks and $\mathcal{O}(10 - 100) \times \sigma_{\text{Tevatron}}$ for sea quarks or gluons case. In the latter case, the ATLAS result gives strong constraint.

Acknowledgement

This work was supported by the World Premier International Research Center Initiative (WPI Initiative), MEXT, Japan. The work of RS and SS is supported in part by JSPS Research Fellowships for Young Scientists.

References

- [1] T. Aaltonen *et al.* [CDF Collaboration], Phys. Rev. Lett. **106** (2011) 171801 [arXiv:1104.0699 [hep-ex]].
- [2] M. R. Buckley, D. Hooper, J. Kopp, E. Neil, [arXiv:1103.6035 [hep-ph]]; F. Yu, Phys. Rev. **D83**, 094028 (2011). [arXiv:1104.0243 [hep-ph]]; X. -P. Wang, Y. -K. Wang, B. Xiao, J. Xu, S. -h. Zhu, [arXiv:1104.1161 [hep-ph]]; K. Cheung, J. Song, [arXiv:1104.1375 [hep-ph]]; X. -P. Wang, Y. -K. Wang, B. Xiao, J. Xu, S. -h. Zhu, [arXiv:1104.1917 [hep-ph]]; L. A. Anchordoqui, H. Goldberg, X. Huang, D. Lust, T. R. Taylor, [arXiv:1104.2302 [hep-ph]]; S. Jung, A. Pierce, J. D. Wells, [arXiv:1104.3139 [hep-ph]]; P. Ko, Y. Omura, C. Yu, [arXiv:1104.4066 [hep-ph]]; P. J. Fox, J. Liu, D. Tucker-Smith, N. Weiner, [arXiv:1104.4127 [hep-ph]]; D. -

- W. Jung, P. Ko, J. S. Lee, [arXiv:1104.4443 [hep-ph]]; S. Chang, K. Y. Lee, J. Song, [arXiv:1104.4560 [hep-ph]]; X. Huang, [arXiv:1104.5389 [hep-ph]]; Z. Liu, P. Nath, G. Peim, [arXiv:1105.4371 [hep-ph]]; J. L. Hewett, T. G. Rizzo, [arXiv:1106.0294 [hep-ph]]; A. E. Faraggi, V. M. Mehta, [arXiv:1106.5422 [hep-ph]]; L. Vecchi, [arXiv:1107.2933 [hep-ph]].
- [3] C. Kilic, S. Thomas, [arXiv:1104.1002 [hep-ph]]; A. E. Nelson, T. Okui, T. S. Roy, [arXiv:1104.2030 [hep-ph]]; B. A. Dobrescu, G. Z. Krnjaic, [arXiv:1104.2893 [hep-ph]]; Q. -H. Cao, M. Carena, S. Gori, A. Menon, P. Schwaller, C. E. M. Wagner, L. -T. Wang, [arXiv:1104.4776 [hep-ph]]; B. Dutta, S. Khalil, Y. Mimura, Q. Shafi, [arXiv:1104.5209 [hep-ph]]; L. M. Carpenter, S. Mantry, [arXiv:1104.5528 [hep-ph]]; G. Segre, B. Kayser, [arXiv:1105.1808 [hep-ph]]; T. Enkhbat, X. -G. He, Y. Mimura, H. Yokoya, [arXiv:1105.2699 [hep-ph]]; C. -H. Chen, C. -W. Chiang, T. Nomura, Y. Fusheng, [arXiv:1105.2870 [hep-ph]]; A. Alves, E. R. Barreto, A. G. Dias, [arXiv:1105.4849 [hep-ph]]; J. Fan, D. Krohn, P. Langacker, I. Yavin, [arXiv:1106.1682 [hep-ph]]; J. Evans, B. Feldstein, W. Klemm, H. Murayama, T. T. Yanagida, [arXiv:1106.1734 [hep-ph]]; J. F. Gunion, [arXiv:1106.3308 [hep-ph]]; D. K. Ghosh, M. Maity, S. Roy, [arXiv:1107.0649 [hep-ph]].
- [4] G. Isidori, J. F. Kamenik, Phys. Lett. **B700**, 145-149 (2011). [arXiv:1103.0016 [hep-ph]]; R. Sato, S. Shirai, K. Yonekura, Phys. Lett. **B700**, 122-125 (2011). [arXiv:1104.2014 [hep-ph]].
- [5] L. A. Anchordoqui, W. -Z. Feng, H. Goldberg, X. Huang, T. R. Taylor, Phys. Rev. **D83**, 106006 (2011). [arXiv:1012.3466 [hep-ph]]; E. J. Eichten, K. Lane, A. Martin, [arXiv:1104.0976 [hep-ph]]; H. B. Nielsen, [arXiv:1104.4642 [hep-ph]]; K. S. Babu, M. Frank, S. K. Rai, [arXiv:1104.4782 [hep-ph]]; R. Harnik, G. D. Kribs, A. Martin, [arXiv:1106.2569 [hep-ph]]; Y. Cui, Z. Han, M. D. Schwartz, [arXiv:1106.3086 [hep-ph]]. R. Fok, G. D. Kribs, [arXiv:1106.3101 [hep-ph]];
- [6] V. M. Abazov *et al.* [D0 Collaboration], arXiv:1106.1921 [hep-ex].
- [7] E. Eichten, K. Lane, A. Martin, [arXiv:1107.4075 [hep-ph]].
- [8] “Kinematic Distribution of events in the $115 < M_{JJ} < 175$ GeV region.”
<http://www-cdf.fnal.gov/physics/ewk/2011/wjj/kinematics.html>

- [9] The ATLAS Collaboration, “Invariant mass distribution of jet pairs produced in association with a leptonically decaying W boson using 1.02 fb^{-1} of ATLAS data”, ATLAS-CONF-2011-097,
<http://cdsweb.cern.ch/record/1369206/files/ATLAS-CONF-2011-097.pdf>
- [10] J. Alwall, P. Demin, S. de Visscher, R. Frederix, M. Herquet, F. Maltoni, T. Plehn, D. L. Rainwater *et al.*, JHEP **0709**, 028 (2007). [arXiv:0706.2334 [hep-ph]].
- [11] L. Moneta, K. Belasco, K. Cranmer, A. Lazzaro, D. Piparo, G. Schott, W. Verkerke, M. Wolf *et al.*, PoS **ACAT2010**, 057 (2010). [arXiv:1009.1003 [physics.data-an]].
- [12] J. Alitti *et al.* [UA2 Collaboration], Nucl. Phys. **B400**, 3-24 (1993).
- [13] D. Stump, J. Huston, J. Pumplin, W. -K. Tung, H. L. Lai, S. Kuhlmann, J. F. Owens, for new physics,” JHEP **0310**, 046 (2003). [hep-ph/0303013].